HYPERBOLICITY OF AUGMENTED LINKS IN THE THICKENED TORUS

ALICE KWON AND YING HONG THAM

ABSTRACT. For a hyperbolic link K in the thickened torus, we show there is a decomposition of the complement of a link L, obtained from augmenting K, into torihedra. We further decompose the torihedra into angled pyramids and finally angled tetrahedra. These fit into an angled structure on a triangulation of the link complement, and thus by [5], this shows that L is hyperbolic.

1. INTRODUCTION

Given a twist-reduced diagram of a link K, *augmenting* is a process in which an unknotted circle component (augmentation) is added to one or more twist regions (a single crossing or a maximal string of bigons) of K. The newly obtained link is called an *augmented link* and the newly obtained diagram is called an *augmented link diagram*. See Figure 2.

Adams showed in [2] that given a hyperbolic alternating link K in S^3 the link L obtained by augmenting K is hyperbolic. In this paper we investigate if this statement holds for links in the thickened torus i.e. if L is a link obtained from augmenting a hyperbolic alternating link K in the thickened torus. We define augmenting similarly for links in the thickened torus with their associated link diagram on $\mathbb{T}^2 \times \{0\}$.

Menasco [9] showed that there are decompositions of the complements of alternating links in S^3 into two topological polyhedra, a top polyhedron and a bottom polyhedron. For alternating links K in the thickened torus, Champanerkar, Kofman and Purcell [4] showed that there is a decomposition of the complement of K into objects called torihedra, which we think of as counterparts to Menasco's decomposition for links in the thickened torus; just like Menasco's decomposition, one obtains a top and a bottom torihedron.

In Section 2 we show that for augmented links in the thickened torus (not necessarily fully augmented), one can also obtain a decomposition of the complement into a top and bottom torihedron. In Section 3, we prove that many augmented alternating links in the thickened torus are hyperbolic.

We point out that [7], the first author proved that *fully* augmented links in the thickened torus are hyperbolic, so this paper can be seen as a generalization of that work.

While revising this paper, we learned that [1] proves a generalization of our work here, showing hyperbolicity of generalized augmented links in an arbitrary thickened surface. We note that our approach, based on angle structures, is different from theirs, which is based on topological arguments.

2. AUGMENTED LINKS

TODO Notation section: $I = (-1, 1)$.

Champanerkar, Kofman and Purcell have studied alternating links in the thickened torus [4]. They define a link in the thickened torus as a quotient of a biperiodic alternating link as follows:

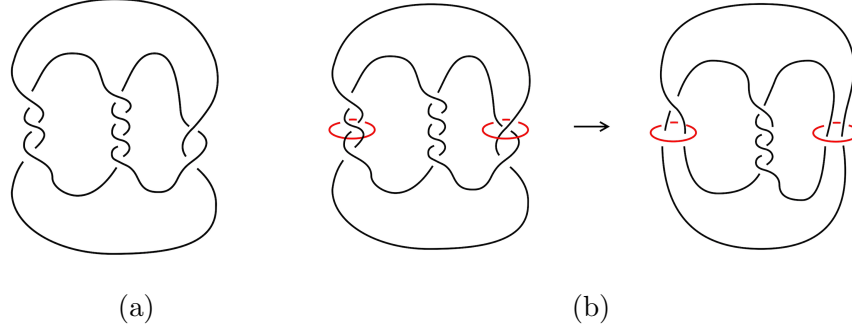(a)   (b)

FIGURE 1. (a) pretzel knot before augmentation (b) pretzel knot after augmentation; second diagram shows removal of full twists in the augmented twist regions.

Definition 2.1. A *biperiodic alternating link* $\mathcal{L}$ is an infinite link in $\mathbb{R}^2 \times I$ with a link diagram $\mathcal{D} \subset \mathbb{R}^2$ such that $\mathcal{L}$ and $\mathcal{D}$ are invariant under the action of a two dimensional lattice Λ on $\mathbb{R}^2$ by translations.

The quotient $L = \mathcal{L}/\Lambda$ is an alternating link in the thickened torus $\mathbb{T}^2 \times I$, whose projection onto $\mathbb{T}^2 \times \{0\} = \mathbb{R}^2 \times \{0\}/\Lambda$ is an alternating link diagram $\mathcal{D}/\Lambda$.

We refer to $\mathbb{T}^2 \times \{0\}$ as the *projection plane*.

Remark 2.2. Since $\mathbb{T}^2 \times I \cong S^3 - H$, where H is a Hopf link. The complement $\mathbb{T}^2 \times I - L = S^3 - (L \cup H)$.

Champanerkar, Kofman and Purcell [4] extended the definition of prime links in S^3 for links in $\mathbb{T}^2 \times I$ called weakly prime.

Definition 2.3. A diagram $D \subset \mathbb{T}^2$ of a link L in the thickened torus $\mathbb{T}^2 \times I$ is *weakly prime* if whenever a disk is embedded in $\mathbb{T}^2$ meets the diagram transversely in exactly two edges, then the disk contains a simple edge of the diagram and no crossings.

Definition 2.4. A *twist region* in a link diagram of $L = \mathcal{L}/\Lambda$ in $\mathbb{T}^2 \times I$, is the quotient of a twist region in the biperiodic link $\mathcal{L}$. A biperiodic link $\mathcal{L}$ is called *twist-reduced* if for any simple closed curve on the plane that intersects the diagram of $\mathcal{L}$ transversely in four points, with two points adjacent to one crossing and the other two points adjacent to another crossing, the simple closed curve bounds a subdiagram consisting of a (possibly empty) collection of bigons strung end to end between these crossings. We say the diagram of L is *twist-reduced* if it is the quotient of a twist-reduced biperiodic link diagram.

Now we can define augmentation for a link in $\mathbb{T}^2 \times I$ the same way we define augmentation for links in S^3:

Definition 2.5. Let $D(K)$ be a twist-reduced diagram of a link K in $\mathbb{T}^2 \times I$. We define *augmenting* as a process in which an unknotted circle component, called a *crossing circle*, is added to one or more twist regions of $D(K)$ (see Figure 2); we call the resulting link L an *augmented link obtained from* K. We say L is *fully* augmented if L is obtained by augmenting K at *every* crossing/twist site.

As pointed out in the introduction, after augmenting a twist region, a standard Dehn twist argument allows us to remove a full twist (that is, two bigons).

FIGURE 2. A: The top right has an odd number of twists while the bottom left has an even number of twists. B: The picture of the link on the right after augmentation twist regions circled in red. C: The link with full twists removed.

Definition 2.6. We say an augmentation has a *half twist* if at least one of the augmented twist regions has an odd number of bigons.

Definition 2.7. A graph $G = (V, E)$ on the torus is *cellular* if its complement is a collection of open disks.

2.1. Torihedral Decomposition of Augmented Alternating Links in Thickened Torus.

We present a method of decomposing an augmented link (not necessarily fully augmented) in the thickened torus into objects called "torihedra" as defined below. Decomposing alternating links in the thickened torus into torihedra were first described in [4], then later used for fully augmented links in the thickened torus in [7]. The idea is to combine methods of Menasco [9] and the use of crossing edges between each crossing of our link and Lackenby's "cut-slice-flatten" method [8] on the augmentation sites.

Definition 2.8. [4] A *torihedron* $\mathcal{T}$ is a cone on the torus, i.e. $\mathbb{T}^2 \times [0,1]/(\mathbb{T}^2 \times \{1\})$, with a cellular graph $G = G(\mathcal{T})$ on $\mathbb{T}^2 \times \{0\}$. The *ideal torihedron* $\mathcal{T}^\circ$ is $\mathcal{T}$ with the vertices of G and the vertex $\mathbb{T}^2 \times \{1\}$ removed. Hence, an ideal torihedron is homeomorphic to $\mathbb{T}^2 \times [0,1)$ with a finite set of points (ideal vertices) removed from $\mathbb{T}^2 \times \{0\}$. We refer to the vertex $\mathbb{T}^2 \times \{1\}$ as the *cone point* of $\mathcal{T}$.

For visualization purposes, we typically draw the graph $G(\mathcal{T})$ of a torihedron from the perspective of the cone point $\mathbb{T}^2 \times \{1\}$. Note however that later we will be dealing with "top" and "bottom" torihedra that are glued together along their torus boundary faces; to avoid confusion, we will visualize the graphs of both torihedra from the perspective of the cone point of the "top" torihedron.

If the faces of $G(\mathcal{T})$ are disks, then $\mathcal{T}$ can be decomposed into a union of pyramids, obtained by coning each face to the cone point of $\mathcal{T}$. This also gives a decomposition of the corresponding ideal torihedron $\mathcal{T}^\circ$ into ideal pyramids. We call these the *pyramidal decompositions* of $\mathcal{T}$ and $\mathcal{T}^\circ$.

Definition 2.9. Let G be a graph with no self-loops on the torus. TODO definition of adding a bow-tie

Proposition 2.10. *Let K be an alternating link in the thickened torus, and let L be an augmented link obtained from K. There is a decomposition of the complement, $(\mathbb{T}^2 \times I) - L$ into two ideal torihedra.*

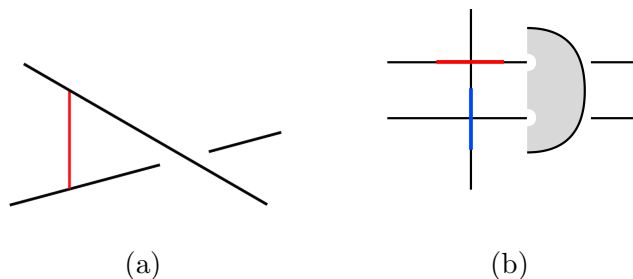(a)   (b)

FIGURE 3. (a) The black strands are part of the link and the red strand is the crossing edge. (b) The blue and red edges represent the split crossing edges and the shaded half disk is bounded by the crossing circle

Proof. We will begin by assuming that L has no half twists. Let $L = K \cup C$, with C being the collection of crossing circles. Arrange L in the following way: place the circle components in C perpendicular to the projection plane $\mathbb{T}^2 \times \{0\}$, and leave the remaining part of the link $K \subseteq L$ lying in the projection plane (except at crossings of K). Thus, the projection of L onto the projection plane will be a diagram $D(K)$ of K together with line segments corresponding to crossing circles. (We demand that $D(K)$ be alternating and twist-reduced.) As discussed before, we may remove full twists (i.e. pairs of bigons) from the twist regions of K that are augmented in L, and since L is assumed to have no half twists, the two edges of $D(K)$ that go through a crossing circle do not meet (see Figure 2 C). From now on, we will take K to be this modified link (with full twists removed).

We now place a *crossing edge* at each crossing of the original link K, connecting the top and bottom strands at the crossing (see Figure 3 (a)).

Next we construct the graph that will define the "top" torihedron. We view the link from the point at infinity from the top end ($\mathbb{T}^2 \times \{1\}$) of the thickened torus. At each crossing of K, push the top strand towards the bottom strand, splitting the crossing edge into two identical edges and spreading them apart as in Figure 3 (b).

Now for each crossing circle c, consider a spanning disk B_c; B_c intersects the projection plane $\mathbb{T}^2 \times \{0\}$ along the red segments in Figure 4, which consists of three edges. We then cut $\mathbb{T}^2 \times I$ along $\mathbb{T}^2 \times \{0\}$ and focus on the top half, $\mathbb{T}^2 \times [0, 1)$. (We will follow the same method on the bottom half to obtain the second identical torihedron.) The spanning disks we placed for each crossing circle are now cut in half along the red segment. Each half of the disk is now bounded by the projection plane and the semi-circle arc of the crossing circle. We push down on the crossing circle and split the half-disk into two identical half-disks. We then push the arc of each crossing circle to infinity, collapsing them to ideal vertices. We obtain two triangular faces which represent the half-disk which look like a bow-tie as in Figure 4 (a). See Figures 5 to 8 for an example.

The crossing edges and edges from spanning disks of crossing circles form the graph of the top ideal torihedron. We repeat the steps for the bottom half of $\mathbb{T}^2 \times I$, $\mathbb{T}^2 \times (-1, 0]$. Thus we get two ideal torihedra.

We obtain the complement of L by gluing the two torihedra with the gluing information given by identifying crossing edges and triangles of the bow-tie. We glue the faces of the torihedra which do not correspond to a bow-tie with a $2\pi/n$ twist where n is the number of sides of each face as in Figure 8 clockwise or counterclockwise.
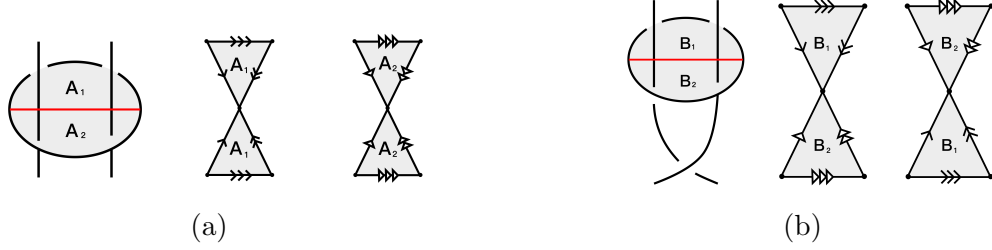
4

FIGURE 4. (a) Gluing of bow-ties without half-twists (b) Gluing with half-twists

Now, if L has half-twists, we apply the constructions above to L', which is the link obtained from L by removing all half-twists (replacing them with parallel strands). The complement of L is again obtained by gluing the torihedra together all the same, except that at the bow-ties coming from twist regions with a half-twist, they are glued as in Figure 4 (b).

For future reference, we will denote the graph for the top and bottom torihedra by $\Gamma_T(L)$ and $\Gamma_B(L)$, respectively, where both graphs are viewed from the cone point of the top torihedron $\mathbb{T}^2 \times \{1\}$. Note that if $L = K$ is the non-augmented link, $\Gamma_T(L)$ is simply the link projection of K, and in fact $\Gamma_T(K) = \Gamma_B(K)$. $\qquad\square$

The Figures 5 to 8 depict an example which decomposes the link (C) of Figure 2.
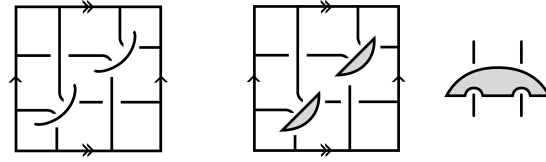

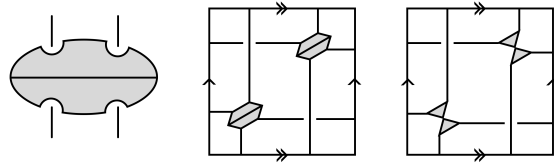FIGURE 5. Each crossing circle bounds a twice-punctured disk

FIGURE 6. We split the disk and collapse the arc of each crossing circle to ideal vertices

Definition 2.11. An *angled torihedron* $(\mathcal{T}, \theta_\bullet^*)$ is a torihedron $\mathcal{T}$ with an assignment $\theta_e^* \in [0, \pi]$ such that for each vertex $v \in G(\mathcal{T})$, $\sum_{e \ni v} \theta_e^* = (\deg(v) - 2)\pi$. We also denote $\theta_e = \pi - \theta_e^*$, so $\sum_{e \ni v} \theta_e = 2\pi$; we refer to θ_e as the exterior angle and θ_e^* as the interior angle. For brevity, we write dihedral angle to mean interior dihedral angle.

We say $(\mathcal{T}, \theta_\bullet^*)$ is *degenerate* if $\theta_e^* = 0$ for some edge; we say it is *non-degenerate* otherwise.
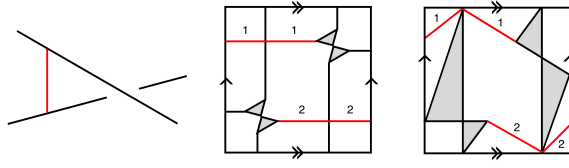
5

FIGURE 7. Left: The crossing arc is the edge in red. Middle: Picture of splitting the crossing edge. Right: The link components are pushed off to infinity.
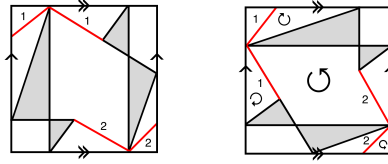

FIGURE 8. Left: The top torihedron. Right: The bottom torihdron with rotation indicating face gluing; TODO shouldn't it be rotating other way.

One may ask for the pyramidal decomposition of a torihedron to "respect" angles. The following definitions, in particular an "angle splitting", make sense of this.

Definition 2.12. An *angled ideal tetrahedron* is an ideal tetrahedron with an assignment of an dihedral angle to each edge, such that

- each dihedral angle is in $[0, \pi]$;
- for each tetrahedron, opposite edges have equal dihedral angles;
- the three distinct interior angles at edges incident to one vertex sum to π.

We say an angled ideal tetrahedron is *degenerate* if one dihedral angle is 0; we say it is *non-degenerate* otherwise.

Definition 2.13. A *base-angled ideal pyramid* is a pyramid whose base is an n-gon, $n \geq 3$, and each boundary edge e_i of the base face is assigned a dihedral angle $\alpha_i \geq 0$ such that the sum is $\sum \alpha_i = 2\pi$. The vertical edge e_i' that meets e_i and e_{i+1} is automatically assigned the dihedral angle $\pi - \alpha_i - \alpha_{i+1}$.

We say a base-angled ideal pyramid is *degenerate* if $\alpha_i = 0$ for some i; we say it is *non-degenerate* otherwise.

Clearly, the dihedral angles of an ideal hyperbolic pyramid make it a base-angled ideal pyramid (with $\alpha_i = \varphi_{e_i}$); it is not hard to see that the converse is true: simply consider a circumsribed polygon such that the side e_i subtends an angle of $2\alpha_i$ at the center, and take the ideal hyperbolic pyramid over it in upper-half space. Also, an angled ideal tetrahedron is simply a base-angled ideal pyramid with base a triangle, and with no preferred face.

Definition 2.14. An *angle splitting* of an angled torihedron $(\mathcal{T}, \theta_\bullet^*)$ is a splitting of $\theta_e^* = \varphi_{\vec{e}} + \varphi_{\overleftarrow{e}}$ for each edge e, where $\vec{e}, \overleftarrow{e}$ are the two orientations on e, such that for each face f, $\sum_{\vec{e} \in \partial f} \varphi_{\vec{e}} = \pi$, where $\vec{e} \in \partial f$ is the edge in the boundary of f taken with outward orientation.
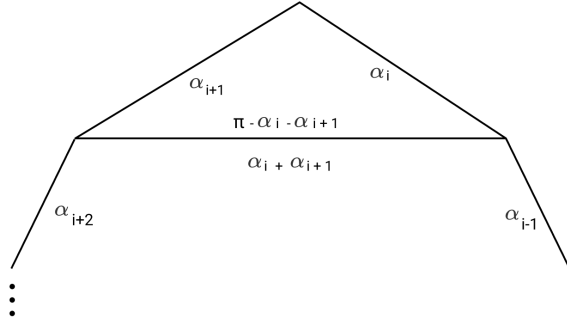
FIGURE 9. Angle-splitting on a polygonal face of the graph

Equivalently, an angle splitting is a decomposition of $\mathcal{T}$ into base-angled pyramids, one for each face of $G(\mathcal{T})$, such that for each boundary edge e of $\mathcal{T}$, the dihedral angles from the two adjacent pyramids add to θ_e^*.

We also say that $\varphi_\bullet$ is an angle-splitting of the edge-labeled graph $(G(\mathcal{T}), \theta_\bullet^*)$.

Remark 2.15. These θ's are related to the θ's in [3], and the φ's are related to their "coherent angle system".

Lemma 2.16. *Let P_n be a base-angled ideal pyramid, and suppose we are given a decomposition of the base face into triangles by adding new edges. One gets an obvious corresponding triangulation of P_n, where a new face is added for each new edge. Then there is an assignment of a dihedral angle to each edge of each ideal tetrahedron in this triangulation such that*

- *each tetrahedron is an angled ideal tetrahedron;*
- *the sum of dihedral angles around each new edge is π;*
- *the dihedral angles of the edges of the original base face are the same as before.*

Proof. Induct on n; there is nothing to prove for the base case $n = 3$.

The proof is essentially given in Figure 9.

Suppose the edges are labeled e_i, for an edge which goes between vertices v_i and v_{i+1}, and suppose e_i is assigned dihedral angle α_i. Let e' be a new edge addeed to the base face of P_n such that it separates the base face into a triangle and an $(n-1)$-gon; suppose the sides of the triangle are e_i, e_{i+1}, and e'. The new face corresponding to e' separates P_n into an ideal tetrahedron T and an ideal pyramid P_{n-1}. We assign the dihedral angle of $\pi - \alpha_i - \alpha_{i+1}$ to e' in T, and assign $\alpha_i + \alpha_{i+1}$ to e' in P_{n-1}. Clearly the sum of dihedral angles condition is satisfied in T and P_{n-1}. It remains to check that the dihedral angles assigned to the vertical (non-base) edges are correct. For the vertical edge associated to v_j for $j \neq i, i+2$, there is nothing to check; for $j = i$, the dihedral angles are $\pi - \alpha_i - (\pi - \alpha_i - \alpha_{i-1})$ in T and $\pi - \alpha_{i-1} - (\alpha_i + \alpha_{i+1})$ in P_{n-1}, which sum to $\pi - \alpha_i - \alpha_{i+1}$; it is similar for $j = i+2$. $\qquad\square$

3. Hyperbolicity of Augmented Links

Thurston introduced a method for finding the unique complete hyperbolic metric for a given 3-manifold M with boundary consisting of tori [10]. Thurston had written down a system of gluing and consistency equations which can be translated to equations with angles
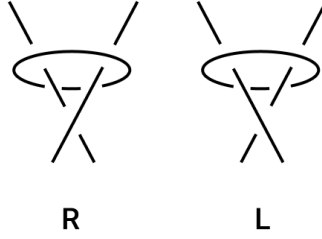
FIGURE 10. R: right augmentation, L: left augmentation

for a triangulation of M whose solutions correspond to the complete hyperbolic metric on the interior of M. Casson and Rivin separated Thurston's gluing equations into a linear and non-linear part [5]. Angle structures is the linear part of Thurston's gluing equations, and what we will use to attain hyperbolicity of complements of augmented links in the thickened torus.

Definition 3.1. Let M be an orientable 3-manifold with boundary consisting of tori. An angle structure on an ideal triangulation τ of M is an assignment of a dihedral angle to each edge of each tetrahedron, such that

- each tetrahedron is a non-degenerate angled ideal tetrahedron,
- around each edge of τ, the dihedral angles sum to 2π.

Theorem 3.2. [6, Theorem 1.1] *Let M be a 3-manifold admitting an angle structure. Then M is hyperbolic.*

For a hyperbolic link K in $\mathbb{T}^2 \times I$, we show that the resulting link obtained from augmenting K is hyperbolic. The idea is to start with a graph from the torihedral decomposition of the link K which will give us a graph on each torihedron with an angle assignment of $\pi/2$ for edge [4]. By Proposition 2.10, there is a torihedral decomposition of the complement of the augmented link L. Using those angles from K, we then assign new angles locally to edges of torihedra from a torihedral decomposition of L and decompose them into base-angled pyramids which can be decomposed into tetrahedra, thus obtaining an angle structure on a triangulation.

Definition 3.3. We say an augmentation is *right-augmented* if, when both strands are (locally) oriented so that they cross the augmentation disk in the same direction, the crossing between them is a positive right-handed half-twist. See Figure 10. We say an augmentation is *left-augmented* if it is not right-augmented.

We can recover L from the link diagram of K together with labels at vertices indicating left- or right-augmentation.

We need the following theorem, adapted from [3, Theorem 4], specialized to genus 1 surfaces:

Theorem 3.4. [3, Theorem 4] *Let $\Gamma = (V, E)$ be a graph on the torus, and let $\Gamma^* = (F, E^*)$ be the dual graph, with E^* being naturally identified with E. Let $\theta_\bullet \in (0, \pi)^E$ be a function on the set of edges E that sums to 2π around each vertex of V.*

There exists an angle-splitting of $(\Gamma, \theta_\bullet)$ if and only if the following "cocycle condition" is satisfied:
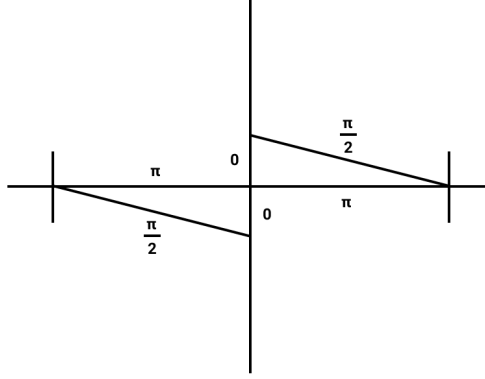
FIGURE 11. Assignments of θ^* to edges of a bow-tie corresponding to an augmentation site

Suppose we cut the torus along a subset of edges in the dual graph Γ^*, obtaining one or more pieces; Then for any piece that is a disc, the sum of $\theta_\bullet$ over the edges in the boundary of the piece is at least 2π, with equality if and only if the piece contains exactly one vertex of Γ.

The original theorem [3, Theorem 4] proves that a circle pattern combinatorially equivalent to Γ exists; a circle pattern naturally yields an angle-splitting (which they call a coherent angle system).

Theorem 3.5. *Let K be a weakly prime, alternating link in the thickened torus whose diagram is cellular and has no bigons. Let L be a link obtained from augmenting K. Then L is hyperbolic.*

More generally, if K is as above with a twist-reduced diagram containing bigons, and L is obtained by augmenting K at every twist region with at least one bigon (and possibly other crossings), then L is hyperbolic.

Proof. Let us first consider the case when K did not have bigons.

By [4, Theorem 7.5], (as discussed in Proposition 2.10,) $\mathbb{T}^2 \times I - K$ can be decomposed into two torihedra $\mathcal{T}_T$ and $\mathcal{T}_B$, with $\mathcal{T}_T$ meeting the top cone point $\mathbb{T}^2 \times \{1\}$ and $\mathcal{T}_B$ meeting the bottom cone point $\mathbb{T}^2 \times \{-1\}$. We denote their graphs by $\Gamma_T(K), \Gamma_B(K)$ respectively; viewed from the top cone point $\mathbb{T}^2 \times \{1\}$, both graphs are the same as the projection graph of K. We make them non-degenerate angled torihedra by assigning $\theta^* = \pi/2$ for all edges.

Using the fact that K is weakly prime, it is not hard to see that the "cocycle condition" of Theorem 3.4 is satisfied.

By Proposition 2.10, $\mathbb{T}^2 \times I - L$ can be obtained by gluing two torihedra $\mathcal{T}_T(L), \mathcal{T}_B(L)$ with graphs $\Gamma_T(L), \Gamma_B(L)$. We make them degenerate angled torihedra by assigning θ^*'s to edges of the bow-ties as in Figure 11, and assign $\pi/2$ to all other edges. It is easy to check that upon gluing, each edge has sum of dihedral angles (θ^*) that is equal to 2π. (This holds true even if they were glued assuming some augmentations had no half-twist; see end of proof where we deal with K having bigons.)

Furthermore, we can obtain an angle-splitting of $\mathcal{T}_T(L)$ (and similarly $\mathcal{T}_B(L)$) by modifying the angle-splitting for $\mathcal{T}_T(K)$; this is shown in Figure 12.
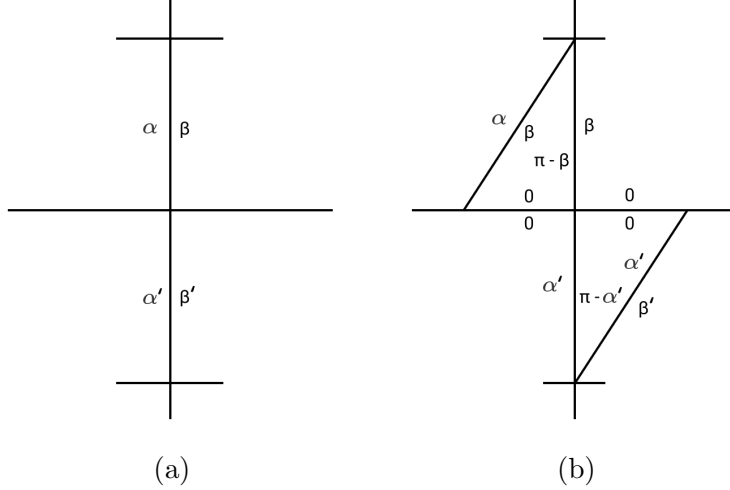
9

FIGURE 12. (a) Angle splitting before augmentation (b) Angle splitting for bowtie corresponding to augmentation

Now we have a decomposition of the two torihedra into degenerate base-angled pyramids. However, we need the pyramids to be non-degenerate, so we first need to modify the angles and graph on the torihedra to make all θ^* nonzero.

Consider a face f of $\Gamma_T(L)$ that is not in a bow-tie. Suppose the corresponding face $\bar{f}$ of Γ, the projection graph (which is equal to $\Gamma_T(K)$), had vertices $v_1, \ldots, v_n$ in counter-clockwise order. We label the edges of f by $e_{i,0}$, $e_{i,\pi}$, or e_i, depending on whether the θ^* is 0, π, or $\pi/2$ respectively, with i non-decreasing from 1 to n, adjacent edges having the same i if and only if they belong to the same bow-tie. For sake of concreteness, suppose that if a vertex v_i is right-augmented, then the augmentation circle intersects $\bar{f}$ (everything is similar if it is left-augmented vertices' circles that intersect $\bar{f}$). In other words, locally, f meets two of the edges of the bow-tie corresponding to a right-augmented vertex v_i (which would be labeled $e_{i,0}, e_{i,\pi}$ in counter-clockwise order), but only meets one of the edges of the bow-tie corresponding to a left-augmented vertex.

Suppose, after cyclically reindexing, $v_1, \ldots, v_k$ is a maximally contiguous subsequence of left-augmented vertices of $G(K)$ around the face $\bar{f}$; the edges around f would start $e_{1,0}, e_{1,\pi}, e_{2,0}, e_{2,\pi}, \ldots$. We add new edges across f as follows. (See Figure 13; ignore the $+$ and $-$ signs for now.)

First suppose $k = n$; then we do nothing.

Next suppose there is only one such maximal contiguous subsequence. If $k = 1$, we add an edge that goes across $e_{1,0}, e_{1,\pi}, e_2$ (in the sense that the new edge separates the edges of f into two sets, one of them being those three edges; since $n \geq 3$, this edge is new). If $k \geq 2$, we add an edge across $e_{1,0}, e_{1,\pi}$ and another edge across $e_{2,0}, e_{2,\pi}, e_{3,0}, \ldots, e_{k,\pi}$ (these two edges do not form a bigon because we've ruled out $k = n$).

Finally, if there are multiple such maximal contiguous subsequences, we just add edges as above for each contiguous subsequence. The only caveat is that if the procedure calls to add a new edge that would form a bigon with the existing edges, we just do not add it.

This way we obtain a new graph $\Gamma_T(L)'$, which defines a new torihedron $\mathcal{T}_T(L)'$. We make $\mathcal{T}_T(L)'$ angled using the angles from $\mathcal{T}_T(L)$ for old edges, and putting π for all new edges TODO make clear it's the red edges that is new.
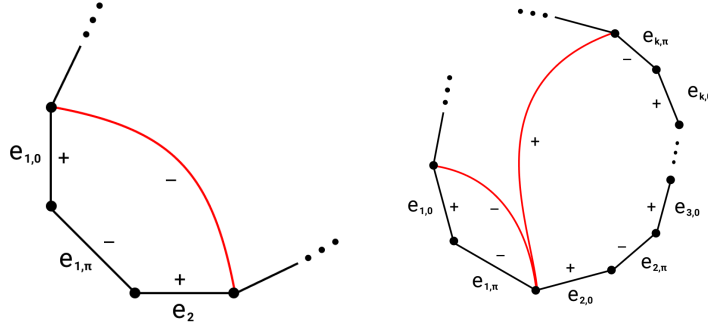
10

FIGURE 13. Red edge indicates an added edge to the graph to appropriately assign +/- labels which indicate increasing/decreasing angles on the edge respectively.

Now we deform the θ^* based on Figure 13, increasing/decreasing by some small $\varepsilon' > 0$ if the edge is labeled $+/-$. Note some edges may be labeled twice, in which case we perform both increasing/decreasing (e.g. if it is labeled $+$ and $-$, the θ^* is not changed). It is easy to see that the sum of θ^* around a vertex remains unchanged. Furthermore, all the edges with θ^* originally equal 0, i.e. all $e_{i,0}$'s, now have positive θ^*, (it receives only one label $+$, because the other face it meets is a bow-tie).

We can directly get an angle-splitting for $\mathcal{T}_T(L)'$ using the angle-splitting for $\mathcal{T}_T(L)$. We reuse the $+/-$ assignments from Figure 13. For $e = e_{i,0}$, we increase $\varphi_{\vec{e}}, \varphi_{\overleftarrow{e}}$ by $\varepsilon'/2$ each; for $e = e_{i,\pi}$, we decrease them by $\varepsilon'/2$ each. For other edges, we increase/decrease $\varphi_{\vec{e}}$ by ε', where $\vec{e}$ is the oriented edge corresponding to the side on which the $+/-$ sign appears in Figure 13; so for example, if an edge e receives both $+$ and $-$, then one of $\varphi_{\vec{e}}, \varphi_{\overleftarrow{e}}$ increases while the other decreases, thus θ_e^* remains constant.

Now we address $\mathcal{T}_B(L)$. In the gluing of $\mathcal{T}_T(L)$ to $\mathcal{T}_B(L)$, non-bow-tie faces of $\Gamma_T(L)$ are identified with non-bow-tie faces of $\Gamma_B(L)$. Under this identification, we add the same edges to $\Gamma_B(L)$, thus obtaining the new torihedron $\mathcal{T}_B(L)'$ with graph $\Gamma_B(L)'$. We perform the same deformations of θ^*'s (or φ's).

We need to check that upon gluing $\mathcal{T}_T(L)'$ to $\mathcal{T}_B(L)'$, the sum of dihedral angles around each edge is still 2π. This was clearly true before deforming, as the new edges of $\Gamma_T(L)'$ only gets identified with the unique corresponding edge of $\Gamma_B(L)'$, and they are both labeled with $\theta^* = \pi$. To see that the deformation does not change these sums, note that in the identification of faces of $\Gamma_T(L)'$ to $\Gamma_B(L)'$, an edge with $\theta^* = 0$ is identified with an edge with $\theta^* = \pi$, so an increase in the former would be conterbalanced by a decrease in the latter. It is also easy to see this is the case for the other edges. (Once again, a similar argument applies if $\mathcal{T}_T(L)'$ and $\mathcal{T}_B(L)'$ are glued assuming some augmentations had no half-twist; see end of proof where we deal with K having bigons.)

Finally, for each face of $\Gamma_T(L)'$ that has more than three sides, we arbitrarily decompose it into triangles and apply Lemma 2.16 to obtain a triangulation of $\mathcal{T}_T(L)'$ into non-degenerate angled tetrahedra; perform the corresponding decomposition for faces of $\Gamma_B(L)'$ and obtain a triangulation of $\mathcal{T}_B(L)'$ into non-degenerate angled tetrahedra. Upon gluing, this gives an angle structure on the triangulation of $\mathbb{T}^2 \times I - L$

11

Now let us consider K with bigons. Let K' be the link obtained from K by replacing each twist region of K by a single appropriate crossing. Let L' be the link obtained from augmenting K' by exactly the same crossing circles. The top and bottom torihedra $\mathcal{T}_T(L'), \mathcal{T}_B(L')$ are the same as $\mathcal{T}_T(L), \mathcal{T}_B(L)$; however, the gluing differs slightly: for twist regions of K that have an even number of bigons, the gluing of $\mathcal{T}_T(L')$ to $\mathcal{T}_B(L')$ should be using Figure 4 (a) (not (b)). As remarked throughout the proof, all the arguments carry through verbatim.

If the original link K had some twist regions with at least one bigon, we may consider augmentations L where all such twist regions are augmented, i.e. L may have augmentations without half-twists. Then, as pointed out in proof of Theorem 3.5 above, the proof still works for L, showing that L is also hyperbolic. $\qquad\square$

References

[1] Colin Adams, Michele Capovilla-Searle, Darin Li, Qiao Li, Jacob McErlean, Alexander Simons, Natalie Stewart, and Xiwen Wang. Generalized augmented cellular alternating links in thickened surfaces are hyperbolic. *arXiv preprint arXiv:2107.05406*, 2021.

[2] Colin C. Adams. Augmented alternating link complements are hyperbolic. In *Low-dimensional topology and Kleinian groups (Coventry/Durham, 1984)*, volume 112 of *London Math. Soc. Lecture Note Ser.*, pages 115–130. Cambridge Univ. Press, Cambridge, 1986.

[3] Alexander I. Bobenko and Boris A. Springborn. Variational principles for circle patterns and Koebe's theorem. *Trans. Amer. Math. Soc.*, 356(2):659–689, 2004.

[4] Abhijit Champanerkar, Ilya Kofman, and Jessica S. Purcell. Geometry of biperiodic alternating links. *J. Lond. Math. Soc. (2)*, 99(3):807–830, 2019.

[5] David Futer and François Guéritaud. From angled triangulations to hyperbolic structures. In *Interactions between hyperbolic geometry, quantum topology and number theory*, volume 541 of *Contemp. Math.*, pages 159–182. Amer. Math. Soc., Providence, RI, 2011.

[6] David Futer and François Guéritaud. From angled triangulations to hyperbolic structures. In *Interactions between hyperbolic geometry, quantum topology and number theory*, volume 541 of *Contemp. Math.*, pages 159–182. Amer. Math. Soc., Providence, RI, 2011.

[7] Alice Kwon. Fully augmented links in the thickened torus. *arXiv preprint arXiv:2007.12773*, 2020.

[8] Marc Lackenby. The volume of hyperbolic alternating link complements. *Proc. London Math. Soc. (3)*, 88(1):204–224, 2004. With an appendix by Ian Agol and Dylan Thurston.

[9] William W. Menasco. Polyhedra representation of link complements. In *Low-dimensional topology (San Francisco, Calif., 1981)*, volume 20 of *Contemp. Math.*, pages 305–325. Amer. Math. Soc., Providence, RI, 1983.

[10] W. P. Thurston. The geometry and topology of three-manifolds. Princeton Univ. Math. Dept. Notes. Available at http://www.msri.org/communications/books/gt3m. [2, 21, 50, 58, 68, 87, 89, 94, 97, 99, 138, 196], 1979.